Thin-Walled Structures **21** (1995) 17–30

0263-8231/95/$9.50

A New Formulation for the Vibration Analysis of a Cylindrical Vessel Containing Fluid via the Use of Artificial Spring Systems

L. Cheng & M. J. Richard

Department of Mechanical Engineering, Université Laval, Québec, Canada G1K 7P4

(Received 22 December 1992; accepted 3 May 1993)

ABSTRACT

This paper presents a new approach for the vibration analysis of cylindrical vessels containing fluid. A new formulation using artificial spring systems at the junction of the shell and end cap was established with the inclusion of the structure–fluid coupling. The method was shown to be well adapted to handle combined structures with the presence of a fluid. Numerical results showed the accuracy of the method as well as the fluid effects on the dynamic behavior of the structure.

INTRODUCTION

Vibration analysis of structures containing fluid has been a topic of major interest to many authors and to the industrial market. When the fluid is light, such as air, it is generally admitted that the interaction between the structure and the fluid is weak so that the fluid–structural coupling may be neglected as a first approximation. However, when the structure is surrounded by heavy fluid, such as most industrial vessels containing a liquid, the effect of the fluid on the vibration of the structure is so important that analysis should be made with the full coupling taken into account. In the present paper, a new formulation using artificial spring systems is presented to study the case of a cylindrical shell with end caps filled with heavy fluid.

Artificial springs have been widely used in the modeling of the boundary conditions of structures.[1–4] The essence of this technique was to introduce artificial springs at the boundary to simulate different boundary cases by adjusting the stiffness of the springs. By doing this, all or some of the geometrical boundary conditions are eliminated. Therefore, the choice of the admissible functions for the structure displacements becomes much more simple and flexible. Recently, the same idea was introduced in the study of the free vibrations of mechanical coupled structures: structures composed of several components. Cheng *et al.*[5] presented a study on a circular cylindrical shell closed at one end by a flexible plate. In that work, artificial springs were used at the shell–plate junction edge to simulate the mechanical coupling. Almost at the same time, Yuan *et al.*[6] published a paper dealing with straight and curved beams. In these works, it has been shown that the technique was quite convenient and efficient to handle the problem of mechanical coupling. In fact, when using the classical Rayleigh–Ritz method for analyzing such systems, the admissible functions should satisfy not only the geometrical boundary conditions but also the continuity with adjoining components, which is a quite difficult task. In the proposed approach, this continuity is automatically assured by permitting the stiffness of the artificial springs to become very large compared to the stiffness of the system. Moreover, a suitable combination of the stiffness of the springs makes it possible to simulate a very large variety of intermediate coupling cases.

This paper can be considered as a continuation of the previous ones. With a cylindrical shell with end caps, the present paper extends the free vibration analysis previously carried out to include the fluid loading from the enclosed cylindrical cavity. It will be shown that the proposed technique is well adapted to the analysis of fluid-loaded structures. This point is one of the main differences from some of the commonly used methods for joined structures such as the receptance method[7] and the transfer matrix method.[8] In fact, these methods are restricted to vibration analysis *in vacuo* and soon become cumbersome when one wants to deal with the coupling problems, where the structure is coupled to a fluid medium. Hence, this paper first concentrates on the presentation of the formulation and several numerical examples are then presented to show the utility of the model.

DESCRIPTION OF THE STRUCTURAL MODELING

Figure 1a shows the basic structure that was investigated. The model consists of a finite circular cylindrical shell closed by two end caps. The cap at the left end ($x = 0$) is assumed to be a flexible plate and the one at right end ($x = L$) a rigid cap. The only reason for assuming a rigid cap is

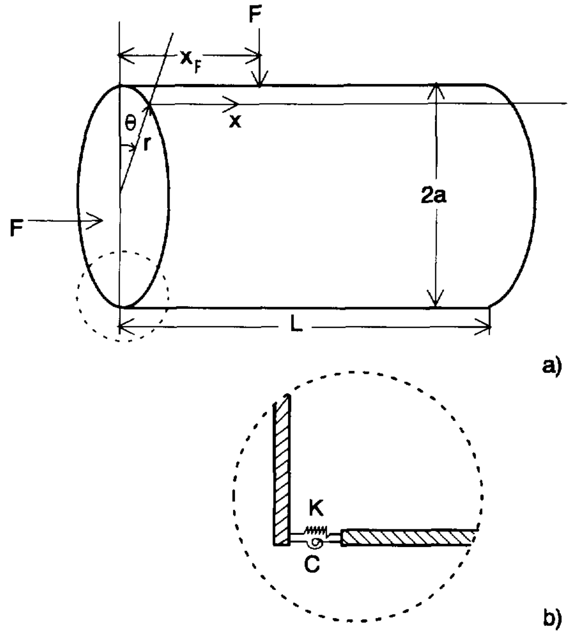

Fig. 1. Investigated structure and spring set-up.

to simplify the presentation and the discussion of the formulation. If this was not the case in practice, the two flexible plates would be treated in exactly the same way presented hereafter. Both shell and plate are assumed to be thin homogeneous structures. The whole structure is assumed to be initially supported by shear diaphragm at each end. The excitation is modeled as a harmonic point load at arbitrary locations situated either on the shell or on the plate.

If the classical Rayleigh–Ritz method was used, one would be faced with a harsh problem: choosing the trial functions satisfying not only the boundary conditions of the plate and the shell, but also the displacement continuity at the junction between them. In order to overcome this difficulty, the whole flexible portion of the structure is considered to be a combination of two substructures (a shell and a plate) connected by two sets of springs as illustrated in Fig. 1b. The figure shows that translational and rotational springs, having respectively distributed stiffness K and C, are added between the shell and the plate along the junction edge. All spring constants are defined in the appropriate units of stiffness per unit length on the contour and are assumed to be constant along the edges.

The governing equations of the plate-ended shell can then be obtained by using the variational principle via the finding of the extremum of Hamilton's function over a suitable subspace of displacement trial functions. A detailed treatment on the free vibration of the structure is given in a previous article.[5] Due to the very lengthy expressions obtained, only an outline is given here with special attention paid to the excitation terms coming from the surrounding field.

The shell displacements u, v and w are decomposed on the basis of the eigenfunctions of a shear diaphragm supported shell as:

$$\begin{Bmatrix} u \\ v \\ w \end{Bmatrix} = \sum_{\alpha=0}^{1} \sum_{n=0}^{\infty} \sum_{m=1}^{\infty} \sum_{j=1}^{3} A_{nmj}^{\alpha}(t)\Pi_{nmj}^{\alpha}(\alpha, n, m, j) \tag{1}$$

where Π_{nmj}^{α} is the eigenvector of the shear diaphragm shell with n and m being, respectively, the circumferential and longitudinal order, α indicates symmetric ($\alpha = 1$) or anti symmetric ($\alpha = 0$) mode and j the type of the modes (bending, twisting, extension–compression); the $A_{nmj}^{\alpha}(t)$ are the coefficients to be determined.

The flexural displacement of the plate w_{p} is expended over a polynomial basis:

$$w_{\mathrm{p}} = \sum_{\alpha=0}^{1} \sum_{n=0}^{\infty} \sum_{m_{\mathrm{p}}=0}^{\infty} B_{nm_{\mathrm{p}}}^{\alpha}(t)\Lambda_{nm_{\mathrm{p}}}^{\alpha}(\alpha, n, m_{\mathrm{p}}) \tag{2}$$

with

$$\Lambda_{nm_{\mathrm{p}}}^{\alpha}(\alpha, n, m_{\mathrm{p}}) = \sin(n\theta + \alpha\pi/2)(r/a)^{m_{\mathrm{p}}} \tag{2a}$$

where n, m_{p}, and α are, respectively, the circumferential order, the radial order and the symmetric index, a is the radius of the plate and the $B_{nm_{\mathrm{p}}}^{\alpha}(t)$ are the coefficients to be determined.

The Hamilton's function H of the whole system can be expressed as follows:

$$H = \int_{t_0}^{t_1} (T_{\mathrm{c}} - E_{\mathrm{c}} + T_{\mathrm{p}} - E_{\mathrm{p}} - E_{\mathrm{k}} + E_{\mathrm{F}})\,\mathrm{d}t \tag{3}$$

where t_0 and t_1 are arbitrary times, T_{c} and T_{p} are, respectively, the kinetic energy of the cylindrical shell and the plate, E_{c} and E_{p} are their potential energies, E_{k} represents the potential energy stored in the springs and E_{F} the work done by the driving forces, including fluid loading from the cavity.

The governing equations of the plate-ended shell are obtained by using the variational principle via the finding of the extremum of Hamilton's function over the trial functions previously chosen. This can be done by using the classical Lagrange equations. Assuming that $A_{nmj}^{a}(t) = A_{nmj}^{a}\exp(j\omega t)$ and $B_{nm_{\mathrm{p}}}^{\alpha}(t) = B_{nm_{\mathrm{p}}}^{\alpha}\exp(j\omega t)$, in which ω is the angular frequency, this procedure yields

$$M_{nmj}(\omega_{nmj}^2(1+j\eta_c)-\omega^2)A_{nmj}^\alpha+\sum_{m'=1}^{\infty}\sum_{j'=1}^{3}X_{nmjm'j'}^\alpha A_{nm'j'}^\alpha$$
$$-\sum_{m_p=0}^{\infty}Y_{nmjm_p}^\alpha B_{nm_p}^\alpha$$
$$=-(F_{nmj}^\alpha)_{\text{shell}}+(P_{nmj}^\alpha)_{\text{shell}} \tag{4}$$

$$\sum_{m'_p=0}^{\infty}(R_{nm_pm'_p}^\alpha(1+j\eta_p)-\omega^2M_{nm_pm'_p}^\alpha)B_{nm'_p}^\alpha+\sum_{m'_p=0}^{\infty}Z_{nm_pm'_p}^\alpha B_{nm'_p}^\alpha$$
$$-\sum_{m=1}^{\infty}\sum_{j=1}^{3}Y_{nmjm_p}^\alpha A_{nmj}^\alpha$$
$$=(F_{nm_p}^\alpha)_{\text{plate}}-(P_{nm_p}^\alpha)_{\text{plate}} \tag{5}$$

In the above expressions, ω_{nmj} and M_{nmj} are, respectively, the natural frequencies and the generalized modal masses of the shear diaphragm supported shell. $R_{nm_pm'_p}^\alpha$ and $M_{nm_pm'_p}^\alpha$ are the stiffness and mass terms of the plate and finally, $X_{nmjm'j'}^\alpha$, $Y_{nmjm_p}^\alpha$ and $Z_{nm_pm'_p}^\alpha$ are the coupling terms via different spring systems. Detailed expressions for the calculations of these terms have been given in Ref. 5. Also in the above expressions, the structural damping factors, η_c and η_p, have been introduced for the shell and the plate, respectively. On the right-hand side of the equations, one notices the direct excitation terms $(F_{nmj}^\alpha)_{\text{shell}}$ and $(F_{nm_p}^\alpha)_{\text{plate}}$ and the fluid loading terms from the cavity $(P_{nmj}^\alpha)_{\text{shell}}$ and $(P_{nm_p}^\alpha)_{\text{plate}}$. They are expressed as:

$$(F_{nmj}^\alpha)_{\text{shell}}=\int_{S_1}F\delta(M-M_F)[\Pi_{nmj}^\alpha]_W\,\mathrm{d}S_1; \qquad M\in S_1 \tag{6}$$

$$(F_{nm_p}^\alpha)_{\text{plate}}=\int_{S_2}F\delta(M-M_F)\Lambda_{nm_p}^\alpha\,\mathrm{d}S_2; \qquad M\in S_2 \tag{7}$$

$$(P_{nmj}^\alpha)_{\text{shell}}=\int_{S_1}P_c[\Pi_{nmj}^\alpha]_W\,\mathrm{d}S_1 \tag{8}$$

$$(P_{nm_p}^\alpha)_{\text{plate}}=\int_{S_2}P_c\Lambda_{nm_p}^\alpha\,\mathrm{d}S_2 \tag{9}$$

In the above expressions, P_c is the fluid pressure inside the cavity; F is the mechanical driving force acting at the point M_F either on the shell surface S_1 or the plate surface S_2; $[\Pi_{nmj}^\alpha]_W$ is the w component of the eigenvector Π_{nmj}^α.

MODELING OF THE FLUID

Let the cylindrical cavity occupy a volume V, and if the fluid within the cavity is assumed to be compressive, non viscous and at rest prior to motion of the wall, the fluid pressure P_c satisfies the familiar wave equation, and associated boundary condition:

$$\nabla^2 P_c + \left(\frac{\omega}{c}\right)^2 P_c = 0 \tag{10}$$

$$\begin{aligned} \frac{\partial P_c}{\partial r} &= -\rho\omega^2 w, \qquad \text{at } r = a \\ \frac{\partial P_c}{\partial x} &= \rho\omega^2 w_p, \qquad \text{at } x = 0 \\ \frac{\partial P_c}{\partial x} &= 0, \qquad \text{at } x = L \end{aligned} \tag{11}$$

In these expressions ρ and c are the equilibrium fluid density and propagation velocity within the cavity. Note that w_p is assumed positive along the positive x-axis.

Equation (10) has normal mode solutions with rigid wall Φ_N with the following properties:

$$\nabla^2 \Phi_N + \left(\frac{\omega_N}{c}\right)^2 \Phi_N = 0 \tag{12}$$

$$\frac{\partial \Phi_N}{\partial \vec{n}} = 0 \tag{13}$$

$$M_N \delta_{NM} = \frac{1}{V}\int_V \Phi_N \cdot \Phi_M \, \mathrm{d}V \tag{14}$$

where Φ_N is the Nth cavity mode and ω_N its related natural frequency; δ_{NM} the Kronecker delta function, $\vec{n}$ is unit vector normal to the corresponding surface (positive toward the outside).

The wave equation (10) can then be transformed into a set of ordinary differential equations by using Green's Theorem in the form

$$\int_V (P_c \nabla^2 \Phi_N - \Phi_N \nabla^2 P_c)\, \mathrm{d}V = \int_S \left(P_c \frac{\partial \Phi_N}{\partial \vec{n}} - \Phi_N \frac{\partial P_c}{\partial \vec{n}}\right) \mathrm{d}S \tag{15}$$

with $S = S_1 + S_2$. One decomposes the fluid pressure P_c on the basis of cavity modes as

$$P_c = \rho c^2 \sum_{N=1}^{\infty} P_N \Phi_N / M_N \tag{16}$$

Substituting expressions (10) to (14) and the decomposition series (16) into equation (15) yields

$$(\omega_N^2 - \omega^2)P_N = (S/V)\omega^2 w_N, \qquad S = S_1 + S_2 \tag{17}$$

in which

$$w_N = -\frac{1}{S}\int_{S_1} w\Phi_N \,\mathrm{d}S_1 + \frac{1}{S}\int_{S_2} w_\mathrm{p}\Phi_N \,\mathrm{d}S_2 \tag{17a}$$

As far as cylindrical cavity is concerned, each mode is represented by four indices: α, n, p and q. Consequently, the mode index N used above will be replaced by the combination of α, n, p, q modal indices. The mode shape and the corresponding angular frequency are

$$\Phi_{npq}^{\alpha} = \sin(n\theta + \alpha\pi/2)J_n(\lambda_{np}r)\cos[(q\pi/L)x] \tag{18}$$

$$\omega_{npq} = c[\lambda_{np}^2 + (q\pi/L)^2]^{1/2} \tag{19}$$

where α is the symmetric index, n the circumferential order, J_n the nth order Bessel function, q the longitudinal order, and λ_{np} the pth root of the following equation:

$$J_n'(\lambda_{np}a) = 0 \tag{20}$$

Considering the displacement decomposition of the structure (expressions (1) and (2)), together with expressions (17a) and (18), eqn (17) becomes

$$(\omega_{npq}^2 + j\eta_v\omega_{npq}\omega - \omega^2)P_{npq}^{\alpha}$$

$$= (\omega^2 S/V)\left[\sum_{m=1}^{\infty}\sum_{j=1}^{3} L^{\mathrm{shell}}(\alpha,n,q,m)A_{nmj}^{\alpha} - \sum_{m_\mathrm{p}=0}^{\infty} L^{\mathrm{plate}}(\alpha,n,p,m_\mathrm{p})B_{nm_\mathrm{p}}^{\alpha}\right] \tag{21}$$

In the above expressions, the damping of the fluid is expressed in terms of a modal damping factor η_V. $L^{\mathrm{shell}}(\alpha,n,q,m)$ and $L^{\mathrm{plate}}(\alpha,n,q,m_\mathrm{p})$ are, respectively, the spatial shell–fluid and plate–fluid coupling coefficients defined as follows:

$$L^{\mathrm{shell}}(\alpha,n,q,m) = \frac{1}{S}\int_{S_1} [\Pi_{nmj}^{\alpha}]_W \cdot \Phi_{npq}^{\alpha}\,\mathrm{d}S_1$$

$$L^{\mathrm{plate}}(\alpha,n,p,m_\mathrm{p}) = \frac{1}{S}\int_{S_2} \Lambda_{nm_\mathrm{p}}^{\alpha} \cdot \Phi_{npq}^{\alpha}\,\mathrm{d}S_2 \tag{22}$$

It can be seen from eqn (21) that the vibration of the vessel acts as an excitation source for the surrounding field.

STRUCTURAL EQUATIONS WITH FLUID LOADING

Using the spatial coupling coefficients defined by eqn (22) with the inclusion of the fluid pressure decomposition series (16), the fluid loading terms appearing on the right-hand side of eqns (4) and (5) can then be expressed by the following expressions:

$$(P^{\alpha}_{nmj})_{\text{shell}} = \frac{\rho c^2 S^2 \omega^2}{V}\left[\sum_{m'=1}^{\infty}\sum_{j'=1}^{3}\sum_{p=1}^{\infty}\sum_{q=0}^{\infty}\frac{L^{\text{shell}}(\alpha,n,q,m)L^{\text{shell}}(\alpha,n,q,m')}{(\omega^2_{npq}+j\eta_v\omega_{npq}\omega-\omega^2)M^{\alpha}_{npq}}A^{\alpha}_{nm'j'} - \sum_{m_{\text{p}}=0}^{\infty}\sum_{p=1}^{\infty}\sum_{q=0}^{\infty}\frac{L^{\text{shell}}(\alpha,n,q,m)L^{\text{plate}}(\alpha,n,q,m_{\text{p}})}{(\omega^2_{npq}+j\eta_v\omega_{npq}\omega-\omega^2)M^{\alpha}_{npq}}B^{\alpha}_{nm_{\text{p}}}\right] \tag{23}$$

$$(P^{\alpha}_{nm_{\text{p}}})_{\text{plate}} = \frac{\rho c^2 S^2 \omega^2}{V}\left[-\sum_{m=1}^{\infty}\sum_{j=1}^{3}\sum_{p=1}^{\infty}\sum_{q=0}^{\infty}\frac{L^{\text{plate}}(\alpha,n,q,m_{\text{p}})L^{\text{shell}}(\alpha,n,q,m)}{(\omega^2_{npq}+j\eta_v\omega_{npq}\omega-\omega^2)M^{\alpha}_{npq}}A^{\alpha}_{nmj} + \sum_{m'_{\text{p}}=0}^{\infty}\sum_{p=1}^{\infty}\sum_{q=0}^{\infty}\frac{L^{\text{plate}}(\alpha,n,q,m_{\text{p}})L^{\text{plate}}(\alpha,n,q,m'_{\text{p}})}{(\omega^2_{npq}+j\eta_v\omega_{npq}\omega-\omega^2)M^{\alpha}_{npq}}B^{\alpha}_{nm'_{\text{p}}}\right] \tag{24}$$

Equations (23) and (24) allow the elimination of the fluid-loading terms appearing at the right-hand side of the coupling equations (4) and (5) and obtain two sets of structural equations. This procedure yields

$$M_{nmj}(\omega^2_{nmj}(1+j\eta_c)-\omega^2)A^{\alpha}_{nmj} + \sum_{m'=1}^{\infty}\sum_{j'=1}^{3}X^{\alpha}_{nmjm'j'}A^{\alpha}_{nm'j'} - \sum_{m_{\text{p}}=0}^{\infty}Y^{\alpha}_{nmjm_{\text{p}}}B^{\alpha}_{nm_{\text{p}}} - \sum_{m'=1}^{\infty}\sum_{j'=1}^{3}\sum_{p=1}^{\infty}\sum_{q=0}^{\infty}\beta^{\alpha}_{npqmm'jj'}A^{\alpha}_{nm'j'} + \sum_{m_{\text{p}}=0}^{\infty}\sum_{p=1}^{\infty}\sum_{q=0}^{\infty}\chi^{\alpha}_{npqmm_{\text{p}}jj'}B^{\alpha}_{nm_{\text{p}}} = -(F^{\alpha}_{nmj})_{\text{shell}} \tag{25}$$

$$\sum_{m'_{\text{p}}=0}^{\infty}(R^{\alpha}_{nm_{\text{p}}m'_{\text{p}}}(1+j\eta_{\text{p}})-\omega^2 M^{\alpha}_{nm_{\text{p}}m'_{\text{p}}})B^{\alpha}_{nm'_{\text{p}}} + \sum_{m'_{\text{p}}=0}^{\infty}Z^{\alpha}_{nm_{\text{p}}m'_{\text{p}}}B^{\alpha}_{nm'_{\text{p}}} - \sum_{m=1}^{\infty}\sum_{j=1}^{3}Y^{\alpha}_{nmjm_{\text{p}}}A^{\alpha}_{nmj} + \sum_{m=1}^{\infty}\sum_{j=1}^{3}\sum_{p=1}^{\infty}\sum_{q=0}^{\infty}\chi^{\alpha}_{npqmm_{\text{p}}jj'}A^{\alpha}_{nmj} - \sum_{m'_{\text{p}}=0}^{\infty}\sum_{p=1}^{\infty}\sum_{q=0}^{\infty}\gamma^{\alpha}_{npqm_{\text{p}}m'_{\text{p}}}B^{\alpha}_{nm'_{\text{p}}} = -(F^{\alpha}_{nm_{\text{p}}})_{\text{plate}} \tag{26}$$

with

$$\beta^{\alpha}_{npqmm'jj'} = \frac{L^{\text{shell}}(\alpha, n, q, m)L^{\text{shell}}(\alpha, n, q, m')}{\lambda^{\alpha}_{npq}}$$

$$\chi^{\alpha}_{npqmm_{\text{p}}jj'} = \frac{L^{\text{shell}}(\alpha, n, q, m)L^{\text{plate}}(\alpha, n, q, m_{\text{p}})}{\lambda^{\alpha}_{npq}}$$

$$\gamma_{npqm_{\text{p}}m'_{\text{p}}} = \frac{L^{\text{plate}}(\alpha, n, p, m_{\text{p}})L^{\text{plate}}(\alpha, n, p, m'_{\text{p}})}{\lambda^{\alpha}_{npq}}$$

$$\lambda^{\alpha}_{npq} = \frac{\rho c^2 S^2 \omega^2}{V(\omega^2_{npq} + j\eta_v \omega_{npq}\omega - \omega^2)M^{\alpha}_{npq}} \tag{27}$$

REMARKS AND NUMERICAL EXAMPLES

Equations (25) and (26) can be used to handle two kinds of problems. Firstly, neglecting the right-hand side that represents exterior excitations, a modal analysis can be performed by solving the eigenvalue equations. The solution gives the natural frequencies of the fluid-loaded structure together with the coefficients for constructing the corresponding mode shapes. Secondly, with the consideration of exterior excitations, a full coupling analysis can be done by solving the whole system. This analysis predicts structural response to exterior loading. In both cases, a truncation of the expansion series (1), (2) and (16) to a finite order is required prior to the numerical procedure.

The general criterion for truncating the series is to increase the terms used in each series until a converged solution is reached. For fluid pressure series, a preliminary estimation of the pressure modes inside the cavity provides a good starting point for the truncation. All modes whose natural frequencies are included within the frequency of interest should be considered. In addition, the inclusion of several higher-order modes is also suggested to cover eventual coupling with the terms kept for the structure. The same principle can be followed for the shell decomposition, in spite of the fact that the modes of a shear diaphragm supported shell constitute only a rough estimation of the shell motion. The polynomial series for the plate is far less physical than the two series mentioned above. Consequently, after the truncation is carried out for the shell and fluid pressure, the number of terms used for the plate is increased until a relatively stable solution is obtained.

Equations (25) and (26) show an interesting feature regarding both structural coupling and structure–fluid coupling. As a matter of fact, only the terms with the same circumferential order n are coupled. This observation suggests that numerical calculation be performed for every given n. In the case of responsive prediction, the solution can be obtained by superposing the response for every n considered. This procedure considerably reduces the amount of calculations and working space. It should be noted that this selective coupling manner is directly due to the symmetry of the structure.

For illustrative purposes, several numerical results are reported in the following sections. Two dimensional stiffness parameters for the springs are defined with comparison to the flexural stiffness of the cylindrical shell D_p as follows: $\bar{K} = Ka^3/D_p$, $\bar{C} = Ca/D_p$. In all the calculations carried out, both values are set to be 10^8 to simulate rigid joint between the shell and the end cap. All other parameters used are tabulated in Table 1.

Example 1: Natural frequencies of a structure containing water

Calculations on the natural frequencies of the same structures *in vacuo* have been reported in a previous publication.[5] In that paper, the accuracy and the efficiency of the proposed formulation has been shown to exist via a comparison with a finite element analysis. In Table 2, the same comparison is reported between the present study and finite element analysis for several lower-order modes of a structure containing water. The natural frequencies of the same structure but *in vacuo* are also given to show the influence of the fluid density. For the finite element model, a 20 × 20 mesh was used for the shell and a 20 × 8 mesh for the end cap. Internal fluid loading is calculated by collocation method.[9] It can be seen that the natural frequencies obtained using the present model agree closely with those using finite element method with a maximum difference of 4%. Moreover, the present method was found to be less time-consuming than the finite element method. For the present case, a time ratio of about 30 was observed.

TABLE 1
Numerical Data Used in Calculations

Structure	*Material*	*Fluid*	*Damping*
Length: $L = 1{\cdot}2$ m	$E = 7 \times 10^{10}$ N/m^2	air: $\rho = 1{\cdot}2$ Kg/m^3	$\eta_c = 0{\cdot}01$
Radius: $a = 0{\cdot}3$ m	$\rho_s = 2700$ Kg/m^3	$c = 340$ m/c	$\eta_p = 0{\cdot}01$
Thickness: $h = 3$ mm	$\nu = 0{\cdot}3$	water: $\rho = 1000$ Kg/m^3	$\eta_v = 0{\cdot}01$
Excit. on shell: $x_F = 0{\cdot}35$ m		$c = 1460$ m/c	

TABLE 2
Natural Frequencies of the Structure Containing Water

	Structure in vacuo	*Structure containing water*	
n	*Present study*	*Present study*	*Finite element results*
0	85·5	55·4	54·9
4	157·5	84·8	86·2
3	176·8	125·7	121·9
5	297·5	165·4	172·6
2	282·7	180·0	185·6
6	290·8	189·7	185·5
5	318·8	215·4	223·1

Example 2: Dynamic response due to external excitations

With a unit point driving force, Figs 2 and 3 show the effect of the fluid on the vibration response of the structure. Numerical results are presented in terms of quadratic velocity averaged over the shell surface or the plate surface (presented in dB referenced to $2{\cdot}5 \times 10^{-15}$ m^2/s^2). Structures in air and also structures containing water are compared.

Figures 2 and 3 show, respectively, the structural response to a harmonic driving force applied to the shell surface when the structure contains air (light fluid) and when the structure contains water (heavy fluid). The driving force is applied to the shell surface with $x_F = 0{\cdot}35$ m. Since the structure is symmetric with respect to the longitudinal axis, the circumferential location of the force is of no importance. It is also assumed that the driving force has a unit amplitude with the frequency going from 5 to 1000 Hz. Several interesting points are worth mentioning; (1) Fig. 2 compares the vibration level of the

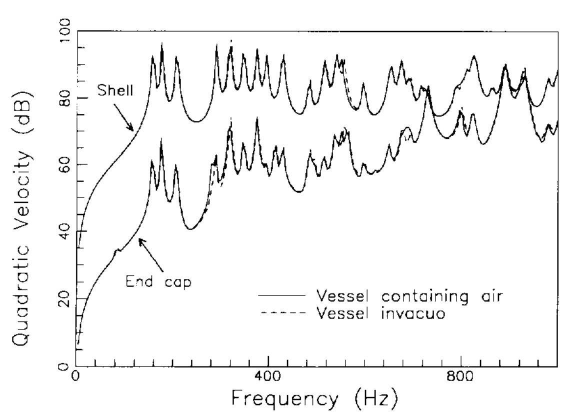

Fig. 2. Quadratic velocity of the vessel in air and *in vacuo*.

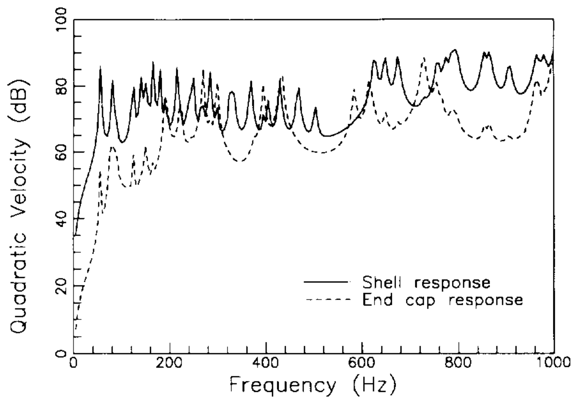

Fig. 3. Quadratic velocity of the vessel containing water.

structure containing air to the case when the fluid is absent. It shows clearly that the presence of air, which is considered to be a light fluid, affects slightly the dynamic behavior of the structure. However, at several resonances, the vibration level of the structure is more or less reduced, indicating that the presence of the air, although light, has a damping effect on the system. It can also be seen from Fig. 2 that the vibration level of the shell is far greater than that of the end cap. All the peaks emerging from the spectra are found to nearly coincide with the natural frequencies of the *in vacuo* structure, meaning that the structure–air coupling is really weak; (2) for the structure containing water, Fig. 3 shows that all the peaks that initially appear in Fig. 2 are shifted significantly to low frequencies, which proves that the coupling between the structure and water is important and that fluid brings non negligible mass effects to the latter. Moreover, because of the presence of the water, the vibration level of the end cap is brought to a comparable level with that of the shell, which is the substructure directly excited. This observation illustrates that mechanical energy generated by the shell is transmitted to the end plate via the fluid. Consequently, the end cap is excited in a more significant manner; (3) by comparing Figs 2 and 3, one can see that the presence of water in the enclosure reduces the vibration level of the shell and, doubtless, brings down the vibration level of the whole structure.

CONCLUSIONS

A new formulation for the vibration analysis of a cylindrical vessel containing fluid is presented in this paper. The use of artificial spring systems between the shell and the end cap facilitates significantly the treatment of the mechanical coupling as well as the structural–fluid coupling. In addition, it permits the use of more physical decomposition series for the structure and the fluid pressure, which contributes to acceleration of calculation speed and guarantees a rapid convergence of the solution. With respect to other methods, this one presents the advantage of being more capable of handling strong coupling of the vessel with the contained liquid.

The utility of the model has been illustrated by two groups of numerical results. The first one shows the accuracy of the method on the prediction of the natural frequencies of the vessel; and the second one shows the effects of the contained liquid on the vibrational behavior of the structure.

The developed technique may be used for other kinds of fluid-containing vessels. However, if the geometry of the structure becomes too complex, or if several substructures should be considered simultaneously, the method may become less appealing, since at each junction, artificial springs are needed. This constitutes the main limitations of the method. One way of overcoming this difficulty may lie in the development of hybrid methods based on the present formulation. The idea is to model the main components of a structure with the developed technique, while the effects of auxiliary components are integrated into the model via other methods. It is expected that this new approach will provide new tools to launch pilot studies and stimulate further research in the field of vibrations applied to industrial vessels.

REFERENCES

1. Pilipich, C. P., Reyes, J. A. & Rossi, R. E., Free vibration of rectangular plates elastically restrained against rotation and translation simultaneously at four edges. *J., Sound Vib.*, **56** (1978) 299–302.
2. Gelos, R. & Laura, P. A. A., Vibrations of an elastically restrained free beam with an intermediate support and carrying concentrated mass. *J. Sound Vib.*, **83** (1982) 139–42.
3. Warburton, G. B. & Edney, S. L., Vibration of rectangular plates with elastically restrained edges. *J. Sound Vib.*, **95** (1984) 537–52.
4. Laura, P. A. A. & Cortiney, V. H., Free vibration of a plate with an inner support. *J. Sound Vib.*, **106** (1986) 409–13.
5. Cheng, L. & Nicolas, J., Free vibration analysis of a cylindrical shell-circular plate system with general coupling and boundary conditions. *J. Sound Vib.*, **155** (1992) 231–47.
6. Yuan, J. & Dickinson, S. M., On the use of artificial springs in the study of the free vibrations of systems comprised of straight and curved beams. *J. Sound Vib.*, **153** (1992) 203–16.
7. Amizi, S., Free vibration of circular plates with elastic edge supports using the receptance method. *J. Sound Vib.*, **120** (1988) 19–35.
8. Irie, T., Yamada, G. & Muramoto, Y., Free vibration of joined conical-cylindrical shells. *J. Sound Vib.*, **95** (1984) 31–9.

9. Lesueur, C., Rayonnement acoustique des structures. Vibroacoustiques, interaction fluide-structure. Collection EDF-DER, Editions Eyrolles, Paris, 1988. Chapter 9, 355–402.
10. Cheng, L. & Nicolas, J., Radiation of sound into a cylindrical enclosure from a point-driven end plate with general boundary conditions. *J. Acoust. Soc. Am.* **91** (1992) 1504–13.